Towards the realization on JET of an integrated H-Mode scenario for ITER

J. Ongena 1*), P. Monier-Garbet 2), W. Suttrop 3), Ph.Andrew 4), M. Bécoulet 2), R. Budny 11), Y.Corre 17) G. Cordey 4), P. Dumortier 1), Th. Eich 5), L. Garzotti 15), D.L. Hillis 12), J. Hogan 12), L.C. Ingesson 6), S. Jachmich 1), E. Joffrin 2), P. Lang 5), A. Loarte 7), P. Lomas 4), G.P. Maddison 4), D. McDonald 4), A. Messiaen 1), M.F.F. Nave 8), G. Saibene 7), R. Sartori 7), O. Sauter 9), J.D. Strachan 10), B. Unterberg 5), M.Valovic 4), I.Voitsekhovitch 19), M. von Hellermann 6), B. Alper 4), Y. Baranov 4), M. Beurskens 4), G. Bonheure 1), J. Brzozowski 10), J. Bucalossi 2), M. Brix 5), M. Charlet 4), I. Coffey 4), M. De Baar 4), P. De Vries 6), C.Giroud 6) C. Gowers 4), N. Hawkes 4), G.L. Jackson 13), C. Jupen 10), A. Kallenbach 3), H.R. Koslowski 5), K.D. Lawson 4), M. Mantsinen 18), G. Matthews 4), F. Milani 4), M. Murakami 12,13), A. Murari 14), R. Neu 3), V. Parail 4), S. Podda 14), M.E. Puiatti 15), J. Rapp 5), E. Righi 7), F. Sartori 4) Y. Sarazin 2), A. Staebler 3), M. Stamp 4), G. Telesca 15), M. Valisa 15) B. Weyssow 16), K.D. Zastrow 4) & EFDA-JET workprogramme contributors[**]

1) LPP / ERM-KMS, Association EURATOM-Belgian State, B-1000 Brussels, Belgium[†]
2) CEA Cadarache, F-13108 St Paul lez Durance, France
3) Max-Planck Institut für Plasmaphysik, EURATOM Association, D-85748 Garching, Germany
4) EURATOM/UKAEA Fusion Association, Culham, UK
5) Institut für Plasmaphysik, Forschungszentrum Jülich GmbH, EURATOM Association, D-52425 Jülich, Germany[†]
6) FOM-Instituut voor Plasmafysica, EURATOM Association, Postbus 1207, NL-3430 BE Nieuwegein, Netherlands[†]
7) EFDA-Close Support Unit, D-85748 Garching, Germany
8) Centro de Fusão Nuclear, Association "EURATOM-IST", 1096 Lisbon, Portugal
9) Centre de Recherches en Physique des Plasmas, Ecole Polytechnique de Lausanne, Association "EURATOM-Confederation Suisse", Lausanne, Switzerland.
10) Chalmers University of Technology, Association "EURATOM-NFR", Göteborg, Sweden
11) Princeton Plasma Physics Laboratory, Princeton University, NJ 08543, USA
12) Oak Ridge National Laboratory, Oak Ridge, TN 37831, USA
13) DIII-D National Fusion Facility, San Diego, CA 92186-5698, USA
14) Associazione EURATOM-ENEA sulla Fusione, Centro Ricerche Frascati, C.P. 65, 00044-Frascati (Rome), Italy
15) Consorzio RFX - Associazione Euratom-Enea sulla Fusione, Corso Stati Uniti 4, I-35127 Padova, Italy
16) Université Libre de Bruxelles, Association "EURATOM-Belgian State", Physique Théorique et Mathématique, Unité de Physique des Plasmas, 1050 Brussels.
17) KTH, Royal Institute of Technology, Association “EURATOM-VR”, Stockholm, Sweden
18) Helsinki University of Technology, Association “EURATOM-Tekes”, Helsinki, Finland
19) Equipe Turbulence Plasmas, PIIM, Universite de Provence, Marseille, France
** See annex in IAEA 2002 J.Pamela IAEA-CN94/OV-1/1.4

e-mail contact of main author : j.ongena@fz-juelich.de

*Researcher at NFSR Belgium
[†] Partners in the Trilateral Euregio Cluster (TEC)

Abstract ELMy H-modes experiments at JET in 2000/mid 2002 have focused on discharges with normalized parameters for plasma density, energy confinement and beta similar to those of the ITER $Q_{DT} = 10$ reference regime ($n/n_{GW} \sim 0.85$, $H_{98(y,2)} \sim 1$, $\beta_N \sim 1.8$). ELMy H-Mode plasmas have been realized reaching or even exceeding those parameters in steady state conditions (up to ~5 s or 12 τ_E) in a reproducible way and only limited by the duration of the additional heating phase. These results have been obtained (a) in highly triangular plasmas, by increasing the average triangularity δ towards the ITER reference value ($\delta \sim 0.5$), and (b) in plasmas at low triangularity ($\delta \sim 0.2$) by seeding of Ar. Pellet injection from the high field side is a third method yielding high density and high confinement, albeit not yet under steady-state conditions. In highly triangular plasmas the influence of input power, plasma triangularity and impurity seeding with noble gases has been studied. Density profile peaking at high densities has been obtained in (a) impurity seeded low triangularity discharges, (b) ELMy H-modes with low levels of input power and (c) discharges fuelled with pellet injection from the high field side. A new ELM behavior has been observed in high triangularity discharges at high density, opening a possible route to ELM heat load mitigation, which can be further amplified by Ar impurity seeding. Current extrapolations of the ELM heat load to ITER show a possible window for Type I ELM operation. Confinement scaling studies indicate an increase of confinement with triangularity and density peaking, and a decrease of confinement with the Greenwald number. In addition, experiments in H isotope and He indicate $\tau_E \propto M^{0.19} Z^{-0.59}$.

The threshold power for the L-H transition in He plasmas shows the same parametric dependence as in D plasmas, but with a 50% higher absolute value.

1. Introduction

The reference scenario for the ITER Q=10 scenario is the ELMy H-Mode with density $n/n_{GW} = 0.85$ (where n_{GW} is the Greenwald density [1] given by $n_{GW}\,[10^{20}m^{-3}] = I_p[MA]/(\pi a^2[m])$, where I_p is the plasma current and a the minor radius of the plasma), energy confinement $H_{98(y,2)} \sim 1$ (where $H_{98(y,2)}$ is the confinement enhancement factor as given by the IPB(98(y,2)) scaling law [2]) and normalized beta value $\beta_N \sim 1.8$ (with $\beta_N = \beta_t\, a[m]\, B_t[T]/I_p[MA]$ and B_t the toroidal magnetic field on axis). A common feature of ELMy H-Mode plasmas is the degradation of confinement with increasing densities, rendering the simultaneous realization of high density and high confinement in such plasmas difficult. Over the past 2 years however we have shown that it is possible on JET to realize the normalized density and confinement parameters for ITER simultaneously with three different methods : (a) by increasing the average plasma triangularity δ to values close to those projected for ITER (Section 2), (b) by extrinsic impurity seeding in low and high triangularity plasmas (Section 3) and (c) with an optimized pellet injection sequence from the high field side in medium δ plasmas (Section 4). Peaked plasma density profiles have been obtained in steady-state conditions in JET with careful tuning of the gas fuelling and plasma heating (Section 5), with impurity seeding and with pellet injection from the high field side, although not yet under stationary conditions. Attention has also been paid to the mitigation of the high divertor power loads that can result during ELMs. Two promising routes, discussed in Section 6, are being explored: (a) high density high triangularity plasmas leading to reduced ELM losses, lower frequency ELMs, and indications for Type II ELMs and (b) seeding of impurities creating a radiating mantle around the plasma. New results on the scaling of the heat load due to ELMs indicate a possibility for Type I operation in ITER. Confinement and L-H power threshold scalings have been refined using the new results and with data from He plasmas in JET (Section 7).

2. High density and high confinement in highly triangular plasmas

Experiments in JET, DIII-D, JT60-U and ASDEX [3-6] have shown the beneficial effect of increasing triangularity to reach high density and high confinement. This study has now been extended on JET [7], by increasing further the average triangularity of the plasmas to values $\delta = 0.47$, close to the ITER

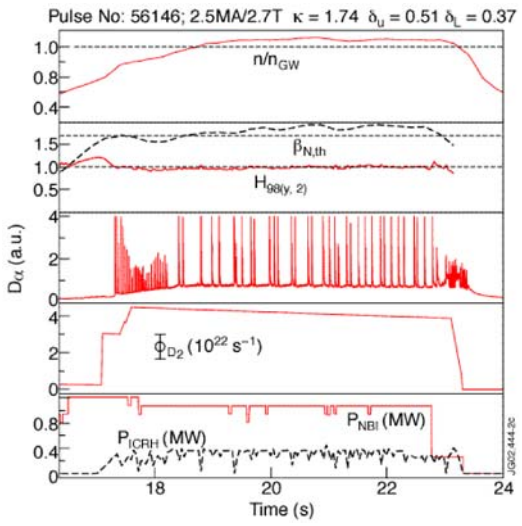

Figure 1: Discharge at high δ reaching simultaneously high confinement, beta and density for about 5 sec.

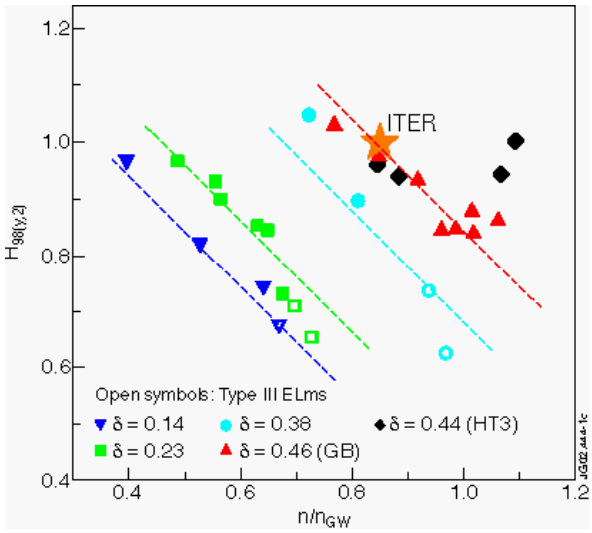

Figure 2: $H_{98(y,2)}$ vs Greenwald factor under stationary conditions for various plasma triangularities.

specifications. Principal plasma parameters of a discharge obtained with high gas puffing into a plasma at $I_p/B_t = 2.5MA/2.7T$ are given in Fig. 1. High δ discharges reach high density ($n/n_{GW} \sim 1.1$, $n \sim 1.10^{20}$ m^{-3}) and confinement ($H_{98(y,2)} \geq 1$, $\beta_N = 1.8$ - 2), exceeding what is required for the Q=10

ELMy H-Mode operation in ITER, simultaneously for a duration of about 4-5 sec, limited only by the length of the heating pulse. Increased confinement is not due to density peaking as plasma density profiles show only a moderate peaking with $n/n_{ped} \sim 1.2$ (with n_{ped} the density measured by the interferometer channel at R = 3.75 m in JET). Due to the carefully designed plasma shape minimizing the vertical forces on the tokamak vessel in the event of a disruption, this configuration is suited for operation at higher plasma currents (up to 3.5MA, possibly 4MA). This is planned in the coming months with the upgrade of the beam heating power in JET to about 22MW. Fig. 2 shows the evolution of the confinement enhancement factor $H_{98(y,2)}$ versus the Greenwald fraction n/n_{GW} for different triangularities studied in JET. Data at the highest triangularities have been obtained in two configurations (i) one matching very closely the projected ITER configuration in the Gas Box Divertor

(upwards pointing triangles) and (ii) in a configuration designed to reduce the disruptive forces (HT3 configuration, diamonds) keeping the same average δ and κ as the ITER configuration, with modified δ_U and δ_L. Data points used for this graph are from discharges heated with NBI heating only, except for the HT3 ones, which were heated by NBI with the addition of up to ~30% ICRH. The enhancement factor $H_{98(y,2)}$ degrades with increasing density for all triangularities, Nevertheless, discharges at low δ can reach similar high performance with pellet injection or impurity seeding (in discharges where the X-point is located on the top of the septum). The best discharges at present are reached at high triangularity and reach simultaneously $n/n_{GW} = 1.1$ and $H_{98(y,2)} \geq 1$. (Note that the confinement data shown here are obtained using an improved equilibrium calculation in JET [8] with respect to earlier publications, but the essential conclusions remain unchanged). Good confinement and density conditions are observed in the presence of Type I ELMs with a reduced ELM size and frequency. A new and interesting ELM behavior has been observed in these high triangularity discharges at high density, opening a new route for ELM mitigation. This will be further discussed in Section 6. At the highest densities, beam deposition profiles become flat or even hollow. Rather stiff electron profiles but less stiff ion temperature profiles are observed. The beneficial effects of high triangularity in reaching high density and confinement in JET could possibly be linked to improved access of the plasma edge to second stability, as seen on other tokamaks e.g. DIII-D [9].

3. Impurity seeding in low and high triangularity plasmas.

Impurity seeding has been successfully applied in TEXTOR, DIII-D, JET and JT-60U over the past years [10] leading not only to high levels of radiation in the edge but also to favorable regimes with enhanced confinement. Work on impurity seeding, started on JET in 1999 [11], has been continued and extended over the past 2 years in plasmas with low and high triangularity [12n-16]. In low triangularity plasmas ($\delta \sim 0.2$), the X-point has been lowered onto the top of the septum, which then plays effectively the role of a limiter. This does not lead to a loss of the H-Mode, but on the contrary, an easier access to the H-Mode is obtained as the L-H power threshold is reduced under such conditions [17], facilitating H-Mode operation at high radiation fractions. The scenario consists of a "puff" and "afterpuff" phase as detailed in [12]. Values in the afterpuff phase reach $n/n_{GW} \sim 0.85$ with confinement $H_{98(y,2)} \sim 1$, representing a significant enhancement in confinement compared to what is otherwise obtained in low triangularity plasmas, for periods of about 5 s or 12 τ_E, only limited by the duration of the heating pulse. For a given temperature, higher densities are reached with impurity seeding in the afterpuff phase with peaking factors up to $n(o)/n_{ped} \sim 1.8$.
Impurity seeding has also been applied to plasmas with high triangularity (configurations similar to the ones of Sect.2) with the X-point well above the dome of the septum. As confinement in these plasmas is less sensitive to strong gas puffing as indicated in Sect. 2, the scenario used in this case does not consist of a "puff" and "after-puff" phase, but a constant deuterium gas puff is applied (Fig. 3), together with a careful dosing of impurities. The figure shows clearly the integrated nature of

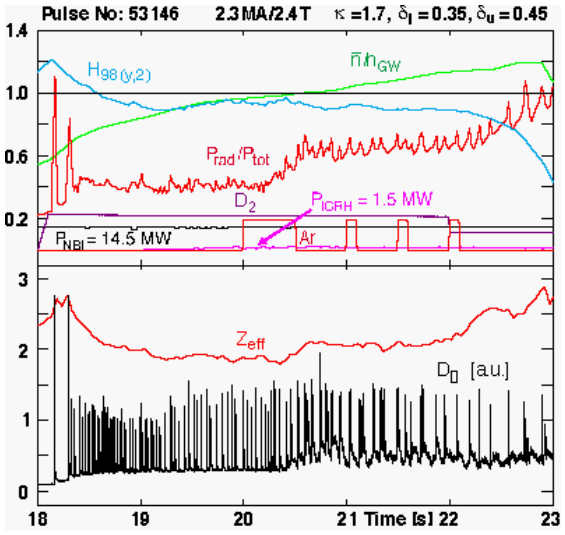

Figure 3: Discharge with Ar seeding at high δ reaching simultaneously high confinement, beta and density for about 5 sec.

these discharges when Ar is present (t > 20s) : (i) high radiation : increased radiation (up to 70%) with formation of a radiating belt (ii) high confinement ($H_{98(y,2)} \sim 0.9$) and thermal $\beta_N \sim 2.1$ (without change in the stored energy of the plasma during Ar seeding) and (iii) high density (up to $n/n_{GW} = 1.2$). IR measurements in the inner and outer divertor show a significant reduction of the power flux to the divertor target plates and therefore of their surface temperature [14]. Note in particular that the change in the character of the ELMs with Ar seeding points to a modification in pedestal parameters, but the global confinement has not changed (See discussion in Sect 6C). For given plasma conditions impurity seeding is thus an additional tool to reduce the detrimental influence of the ELMs, without reduction of confinement. Best conditions are realized when pumping is reduced (and thus recycling is more pronounced). Clear radiating mantles for septum (low δ) and ITER-like (high δ) cases are obtained [18]. Application of central ICRH is beneficial to avoid central impurity accumulation [16]. Depending upon the details of Ar seeding, impurity accumulation can be observed, generally correlated in time with sawtooth suppression and peaking of the impurity profile in the center. The sawtooth suppression is linked to an increase of the value of the central q above unity. Application of on-axis ICRH heating prevents the q(0) value from raising above unity, permitting to keep the high performance phase for the whole heating period.

4. Optimized pellet sequence to reach high density with high confinement.

The potential of high side pellet injection for fuelling the plasma to high densities with simultaneous high confinement has been investigated in ELMy H-Mode discharges in JET [19]. An optimized fuel cycle can avoid too excessive prompt particle losses leading to an increase in the neutral gas pressure and edge density. The optimization strategy consists in a first phase where the density is ramped up (while allowing for a small confinement loss) followed by a second phase minimizing the particle flux in order to maintain the density and to recover confinement. In this way plasma densities could be obtained above the Greenwald with simultaneous high plasma energy content corresponding to $\beta_N > 1.8$.

5. Long time-scale density peaking

Long time-scale density peaking has been observed in JET plasmas at densities exceeding the Greenwald value [20]. These neutral beam heated discharges are characterized by type-I ELMs and good energy confinement. A power scan in 1.9MA/2.0T plasmas shows that at low NBI heating powers ($P_{NBI} < 8$ MW), the plasmas obtained are transient, with a density profile peaking increasing linearly with time, reaching values up to $n(0)/n_{ped} \sim 2$. The central plasma temperature drops, the current profile broadens and sawteeth are lost, followed by a radiative collapse of the plasma center. At high NBI heating powers ($P_{NBI} > 12$ MW), central density is limited by higher m/n = 4/3 Neoclassical Tearing Modes. These limitations can be avoided at intermediate NBI heating levels ($P_{NBI} \sim 10$ MW), sometimes assisted by low power ($P_{ICRH} = 1$-2 MW) centrally deposited ICRH (to mitigate a radiative collapse of the center), and with an optimized gas waveform to reduce the size of the first ELM, to avoid triggering a large m/n = 3/2 NTM, detrimental to confinement. A gas position scan showed that gas puffing from the inner ring into the private divertor region is beneficial for density peaking. In this way plasmas are obtained with $n/n_{GW} = 1$ and with a density peaking $n(0)/n_{ped} \sim 1.3$, at high confinement $H_{98(y,2)} \sim 0.96$ and $\beta_N = 2$.

6. Studies in ELM mitigation

A. Observation of reduced ELM losses at high density and high confinement in high triangularity plasmas without impurity seeding

The decrease of P_{ELM} / P_{IN} at high density is due to the fact that with increasing D puffing the ELM frequency first increases, then reaches a maximum to decline again [21-22]. This new ELM behavior breaks the usual link between f_{ELM} and W_{ELM}, observed at low δ and lower input powers [23], and consequently ELM losses are less at higher densities, leading to values for $H_{98(y,2)} \sim 1$ for densities $n/n_{GW} > 0.9$, as shown in Section 2. The MHD activity appears at high density in between ELMs as an increased level of density and broadband (15-50 kHz) magnetic fluctuations at high poloidal to toroidal periodicity, suggesting edge localization [21], reminiscent of "quasi-coherent" modes associated with EDA Modes in Alcator-C [24] and Type II ELMs in ASDEX-Upgrade [25]. The reduction in $\Delta W_{ELM}/W_{ped}$ (with $\Delta W_{ELM} = W_{dia\ before\ ELM} - W_{dia,\ after\ ELM}$ and $W_{ped} = 3/2\ (n_{e,ped}\ (T_{e,ped} + T_{i,ped}))\ V_p$, where the pedestal values are taken at the top of the H-Mode pedestal just before the ELM and V_p is the confined plasma volume) is mainly entirely due to the reduction in temperature in the pedestal region with the density change due to Type I ELMs nearly independent of the pedestal density. The value of $\Delta T_{e,ped}/T_{e,ped}$ decreases with increasing density and when $\Delta T_{e,ped}/T_{e,ped} \sim 0$ the drop in pedestal pressure due to the ELM is entirely due to the (small) change in pedestal density. A value of $\Delta T_{e,ped}/T_{e,ped} = 0$ is obtained in plasmas with high upper triangularity ($\delta_u \sim 0.5$) and reduced lower triangularity ($\delta_l \sim 0.3$), leading to so-called "minimum" ELMs, with $\Delta W_{ELM}/W_{ped} \sim 4\%$, (at $H_{98(y,2)} \sim 1.05$ and $n/n_{GW} \sim 0.8$), the lowest value obtained so far on JET, and very well within the range required for ITER ($3\% < \Delta W_{ELM}/W_{ped} < 15\%$).

B. ELM mitigation by impurity seeding

For both low and high δ discharges studied, the increase in radiated power due to Ar seeding leads to reduced target loads, with only a minor influence on Z_{eff} (typically $\Delta Z_{eff} \sim 0.2$-0.3), with an increase in density for a given confinement quality (See Sect. 3).

A. Low or medium δ discharges. In the afterpuff of low δ septum discharges, the lower D_2 puffing rate leads usually to a reduced frequency and Type I ELMs. The addition of Ar, further reduces the ELM frequency. Not only the frequency of the ELM is reduced with Ar seeding, but also there is reduction of $\Delta W_{ELM}/W_{ped}$ correlated with increase of edge electron collisionality or ion parallel transit time $\tau_{//front}$ (See Sect 6C). A significant divertor surface temperature reduction due to Ar seeding has been measured by IR thermography of the inner and outer target plates in recent experiments at medium δ [26] (in the so-called DOC configuration especially developed to allow detailed thermographic measurements) as shown in Fig. 4, where data are compared from discharges with roughly the same confinement and core parameters, with and without impurity seeding. Note that not only during the ELM but in particular also in between the ELMs the surface temperature is reduced. This unique feature of Ar seeding will allow for larger temperature excursions due to ELMs without reaching the ablation limit of the target material.

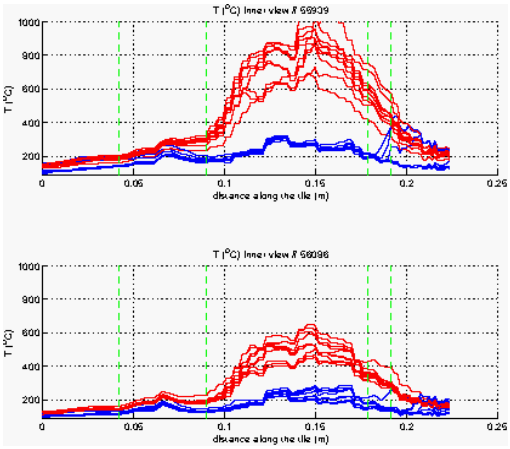

Figure 4: IR temperature profile as a function of the distance along the inner divertor target during (red) and in between (blue) ELMs for an unseeded (top) and Ar seeded (bottom) medium δ discharge.

B. High δ discharges. A radiating belt is formed associated with a significant increase in the radiated power fraction. In addition, Ar seeding also causes a drop in ELM frequency, together with an increase in the base level D_α emission, indicative for an increased recycling between ELMs, resembling the phenomena seen with mixed Type I/II ELMs in unseeded high δ discharges. The ELM frequency is reduced compared with the unseeded reference (see Fig. 3), with almost constant

$\Delta W_{ELM}/W_{ped}$ = 5-7% [14] leading to a reduced divertor load averaged over the ELMs. The strong moderation is also supported by IR heat flux measurements (as in the low δ case) and the marked drop of the electron temperature just in front of the target plates measured with Langmuir probes [15]. A partial detachment of the plasma in the divertor is seen under those conditions. Similar ELM moderation as with Ar seeding can be obtained with strong D puff, but (i) without the beneficial effects of the increase in particle confinement time (leading to a higher density for the same high energy confinement), and (ii) without the formation of a radiating belt, decreasing the overall heat flux towards the target plates.

C. ELM characteristics and plasma parameters

A strong correlation has been found between the Type I ELM size and either the dimensionless electron collisionality at the top of the pedestal or the transit time of the ELM heat front to the target plate (calculated with pedestal parameters) $\tau_{//}^{front}$ [27] for all plasma conditions studied, including impurity seeding and the new Type I ELM behavior described above (see Fig. 5a and 5b). JET has thus shown that the pedestal parameters determine the ELM size, the frequency being determined for a given power flux through the separatrix by the transport in between ELMs in the plasma edge region. [21-22]. The beneficial reduction in ELM size at high gas puffing rates in both high δ plasmas, and plasmas with

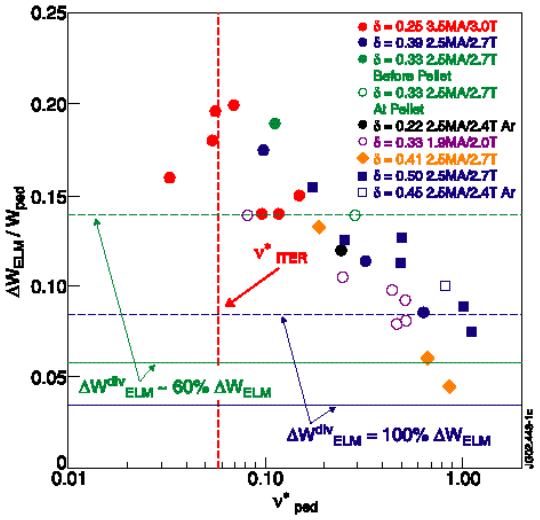

Figure 5a: ELM size versus neoclassical edge collisionality for a wide range of plasma conditions in JET. ELM size limits for ITER are indicated for (i) an inter-ELM load of 5MW/m² and an increased inclination of the divertor targets (dashed lines) and (ii) for an inter-ELM load of 10MW/m² and the ITER reference design for the targets (full lines), assuming that only 60% (green) or 100% (blue) of the bulk plasma energy loss is arriving at the divertor targets [28].

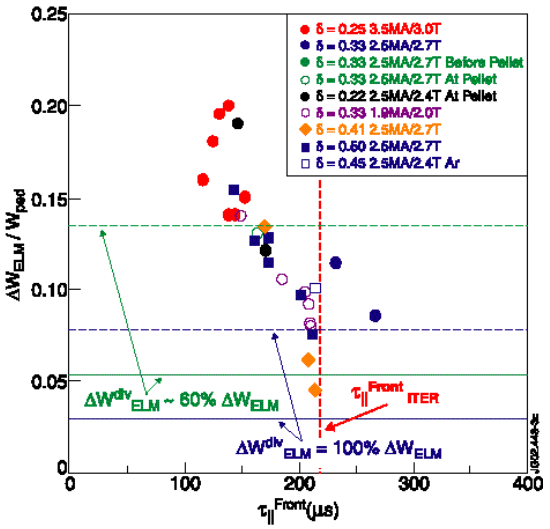

Figure 5b: ELM size versus the transit time of the ELM heat front to the target plate $\tau_{//}^{front}$ for a wide range of plasma conditions in JET. ELM size limits for ITER are indicated for (i) an inter-ELM load of 5MW/m² and an increased inclination of the divertor targets (dashed lines) and (ii) for an inter-ELM load of 10MW/m² and the ITER reference design for the targets (full lines), assuming that only 60% (green) or 100% (blue) of the bulk plasma energy loss is arriving at the divertor targets [28].

impurity seeding can thus be understood as due to the resulting increase of edge collisionality or the increase of $\tau_{//}^{front}$. Fig. 5a and 5b show the present estimate of the acceptable ELM energy in ITER based on divertor lifetime (less that 0.01 μm erosion per ELM) for both experimental correlations and for two assumptions on the ELM energy loss from the bulk plasma that reaches the divertor target. The upper and lower values in these ranges originate from differences in the assumptions on the detail of the ELM power deposition and of the angle of incidence of the field line on the ITER divertor target [33]. In order to determine whether the observed Type I ELMs are extrapolable to next step devices requires not only the knowledge of the bulk plasma energy loss, but also detailed information on the characteristics of the ELM energy flux to the divertor target (proportion of the energy that reaches the divertor target, area over which is deposited, time, etc.). In order to determine whether the observed Type I ELMs are extrapolable to next step devices requires not only the knowledge of the bulk plasma

energy loss, but also detailed information on the characteristics of the ELM energy flux to the divertor target (proportion of the energy that reaches the divertor target, area over which is deposited, time, etc.). In this respect, experiments with ELM time-resolved divertor energy flux have contributed to firm up the basis for the extrapolation of the present results to ITER.

7. Confinement scaling and L-H Power Threshold studies

Several confinement aspects have been studied at JET over the past 3 years. The new results obtained and discussed in Sections 2 to 4 allowed to investigate the influence of peaking, triangularity and proximity to the Greenwald limit on energy confinement [29], variables that are not contained in the current scaling expressions used to predict the performance of ITER. The best fit of the residuals of the ratio $\tau_{E,exp} / \tau_{98(y,2)}$ to a subset of the new data for which accurate pedestal values for n_{ped} were available, was obtained using the variable $F_q = q_{95}/q_{cyl}$ [30] as a shaping parameter, and resulted in a corrected enhancement factor $H_{98(y,2),corr} = F \times H_{98(y,2)}$, where $F = 0.46 + 1.35 \ln(F_q) - 0.17\, n/n_{GW} + 0.38\, (n/n_{ped} - 1)$.

8. Conclusions and Outlook

The experimental campaigns of the last 3 years on JET have resulted in a simultaneous extension of density and confinement in ELMy H-Mode plasmas using various methods. By further increasing the average triangularity of the plasma, discharges have now been realized with values for $H_{98(y,2)} \geq 1$ and $n/n_{GW} \sim 1.1$, which exceeds what is required for the ITER Q=10 standard scenario. The flattop duration of these discharges is about 5s and is only limited by technical constraints on JET. These high density, high confinement discharges exhibit energy losses by other mechanisms than pure ELM activity, and this points to a possible way for ELM mitigation. High density in high δ discharges leads to a reduction in ELM frequency, which is contrary to the usual relation between ELM frequency and ELM size. Detailed analysis of the ELM behavior and additional thermographic measurements on the divertor targets indicate that there is a possible window for operation for Type I ELM discharges in ITER. Impurity seeding is an additional tool to mitigate ELMs in discharges with high and low triangularity and has no detrimental effect on energy confinement or neutron production. Pellet injection from the high field side with a tailored injection rate has also resulted in discharges with high density and high confinement, but more work is needed to optimize the stationarity. Discharges with strong density peaking ($n(0)/n_{ped} \sim 2$) have also been obtained without pellet injection, by careful gas dosing over long time intervals. Density peaking and high β values both favor the destabilization of Neoclassical Tearing Modes (NTMs) due to the associated increased bootstrap current fraction. This can be a limiting factor for the confinement properties of such plasmas, unless care is taken to avoid the creation of large seed islands, induced by e.g. large first ELMs or sawteeth, or by varying the ICRH phasing [31]. Confinement studies show an increase of energy confinement with density peaking and triangularity, but still a degradation of confinement with increasing Greenwald factor. Density peaking and plasma shaping have a beneficial influence on confinement. Confinement scaling studies with data from He discharges confirmed the mass dependence of the IPB98(y,2) scaling, and combined with previous T and H studies, suggest $\tau_E \propto M^{0.19} Z^{-0.59}$. Threshold power studies in He show the same dependence on magnetic field, density and mass as for deuterium, but the absolute value is about 50% higher in He. Extensions of the results presented in this paper to higher currents, fields and heating powers and towards longer flattop durations on JET are prepared [32], in view of a continued preparation for ITER.

References

[1] GREENWALD M., et al., Nucl. Fusion 28 (1998) 2199
[2] ITER Physics Basis, Nucl. Fusion 39 (1999) 2175
[3] OSBORNE T.H., et al., Plasma Phys. Control. Fusion 42 (2000) A175
[4] SAIBENE G., et al., Nucl. Fusion 39 (1999) 1133
[5] SUTTROP W., et al., Plasma Phys. Control. Fusion 42 (2000) A97
[6] KAMADA Y., et al., Fusion Energy 1996 (Proc. 16th Int. Conf. Montreal, 1996), IAEA, Vienna (1997) 247
[7] SAIBENE G., et al., Plasma Phys. Control. Fusion 44 (2002) 1769
[8] CORDEY G., McDONALD D., JET Internal Report; http://users.jet.efda.org/pages/codes-

data/dvcm/Parameters/confinement.htm
[9] LAO L.L., et al., Nucl. Fusion, 41 (2001) 295
[10] ONGENA J., Phys. Plasmas 8 (2001) 2188
[11] STRACHAN J.D. et al., Plasma Phys. Control. Fusion 42 (2000) A81
[12] DUMORTIER P., et al., Plasma Phys. Control. Fusion 44 (2002) 1845
[13] PUIATTI M.E., et al., Plasma Phys. Control. Fusion 44 (2002) 1863
[14] JACHMICH S., et al., Plasma Phys. Control. Fusion 44 (2002) 1879
[15] TOKAR M.Z., et al., Plasma Phys. Control. Fusion 44 (2002) 1903
[16] NAVE, M.F.F., et al., submitted for publication in Nucl. Fusion (2002).
[17] HORTON L. Proc.26th EPS Conf. on Control. Fusion and Plasma Phys. (Maastricht, 1999) paper P1.021 (CD-ROM).
[18] HILLIS D., et al., "Influence of Ar recycling and Divertor Configuration on Confinement in JET radiating discharges", Bull. Amer. Phys. Soc., paper GP1.050 (Proc. 43rd Annual Meeting of the APS Division of Plasma Physics, Long Beach, California, Nov. 2002)
[19] LANG P.T., et al., Plasma Phys. Control. Fusion 44 (2002) 1919; Nucl. Fusion 42 (2002) 388
[20] VALOVIC M., et al., Plasma Phys. Control. Fusion 44 (2002) 1911
[21] BECOULET M., et al., Plasma Phys. Control. Fusion 44 (2002) A103-A112
[22] LOARTE A., et al., Plasma Phys. Control. Fusion 44 (2002) 1815
[23] FISHPOOL G.M., Nucl. Fusion 38 (1998) 1373
[24] GREENWALD M., Phys. Plasmas 6 (1999) 1943
[25] STOBER J., et al., Nucl. Fusion 41 (2001) 1123
[26] RAPP J., et al., "Reduction of Heat Load in JET ELMy H-Modes Using Impurity Seeding Techniques", this conference, paper IAEA-CN94/EX/P1-09
[27] LOARTE A., et al., "Type I ELM energy and particle losses in JET ELMy H-Modes and implications for ITER", this conference, paper IAEA-CN94/EX/P1-08
[28] FEDERICI G., Proc. PSI Conference Gifu (2002), to be published in J.Nucl.Mat.
[29] CORDEY G., et al., Plasma Phys. Control. Fusion 44 (2002) 1929
[30] KARDAUN O.J.F, Plasma Phys. Control. Fusion 41 (1999) 429
[31] SAUTER O., et al., Phys.Rev.Lett 88 (2002) 105001
[32] JOFFRIN E., LOMAS P., personal communication